

## Highly improved adsorption selectivity of L-phenylalanine imprinted polymeric submicron/nanoscale beads prepared by modified suspension polymerization

Nasrullah Shah, Jung Hwan Ha, Mazhar Ul-Islam, and Joong Kon Park<sup>†</sup>

Department of Chemical Engineering, Kyungpook National University, Daegu 702-701, Korea  
(Received 27 January 2011 • accepted 10 March 2011)

**Abstract**—Molecularly imprinted polymer (MIP) submicron/nanoscale beads selective for L-Phenylalanine (L-Phe) and D-Phe as well as non-imprinted beads were prepared by modified suspension polymerization involving agitation of the reaction mixture at high rotation speed under safe radical conditions. The effects of pH, template and concentration of racemate solution on the performance of the phenylalanine (Phe) imprinted polymeric submicron/nanoscale beads were studied. L-Phe-imprinted submicron/nanoscale beads prepared for the first time by modified suspension polymerization showed enhanced adsorption capacity and selectivity over those of D-Phe imprinted and non-imprinted beads. Maximum adsorption capacity, 0.35 mg/g, and selectivity, 1.62, of L-Phe imprinted submicron/nanoscale beads were higher than the adsorption capacities, 0.30 and 0.19 mg/g, and selectivities, 1.59 and 1.02, of D-Phe imprinted and non-imprinted submicron/nanoscale beads, respectively. FE-SEM analyses revealed that L- and D-Phe imprinted beads were larger (100 nm-1.5  $\mu$ m) than non-imprinted nanobeads (100-800 nm). <sup>13</sup>C CP-MAS NMR spectroscopy helped in correlating the bead sizes and the extent of reaction during polymerization. Similarly, FT-IR study was used for evaluation of structural characteristics of the prepared Phe-imprinted and non-imprinted beads. The preparation of Phe-imprinted submicron/nanoscale beads with improved adsorption and separation properties and the study of effect of template on the size and performance of the prepared beads are suitable from both economical and research point of view in MIP field.

Key words: Molecularly Imprinted Submicron/Nanoscale Beads, Modified Suspension Polymerization, FE-SEM, FT-IR, <sup>13</sup>C CP-MAS NMR

### INTRODUCTION

Molecular imprinting has been used for synthesizing polymeric substances carrying specific binding sites having high affinity towards chiral compounds, drugs, peptides and proteins, etc. [1-7]. The synthesis of small MIPs is of great importance. The preparation of nanoscale MIPs is gaining importance due to small sizes and large number of features per volume. Due to smaller sizes the binding sites are situated at or near the material's surface, which minimizes the diffusion distances of molecules and results in high performance of the MIPs [8-13]. The dispersion of MIP nanomaterials in analyte solution and the removal of template are easy [7,14-16]. The nanoscale MIPs are applicable in different fields such as in the construction of biosensors, drug delivery systems or in the development of new material for separation and purification purposes. Large MIP particles may also be employed for such applications, but due to low mass transfer and low separation ability these are not suitable for obtaining rapid separations [14].

Considering the importance of small-sized MIPs, submicron and nanosized MIPs in different formats were tried by different researchers [4,7-9,12,17,18]. However, most of these nanoscale MIP formats employ relatively long and complicated procedures [4,7,8,12] or suffer from lower uptake capacity [18] and some involve high agglomeration of the prepared MIP particles/beads [9]. For instance,

nanosized MIPs were prepared using the surface modified alumina membrane. However, the modification of alumina and polymerization within the available pores made the process complicated and time consuming [4,7,8,12]. Zhu et al. [9] prepared submicron scaled particles selective for 17- $\beta$ -estradiol by using precipitation polymerization and used in the HPLC column. However, the extent of agglomeration was very high. Nanosized S-propranolol imprinted nanoparticles were prepared using the mini-emulsion polymerization as was done by Priego-Capot et al. [18]. However, the uptake capacity of the imprinted nanoparticles was 10 times lower than that of the propranolol-imprinted microspheres prepared by precipitation polymerization.

Compared to these methods, suspension polymerization using simple agitation is convenient for the production of round MIP beads with suitable size distribution. According to our knowledge and literature study, the modified suspension polymerization was not tried yet for the preparation of MIP submicron/nanoscale beads for the resolution of underivatized phenylalanine racemic mixture. In a previous study Khan and Park [16] attempted to reduce the size of the D-phenylalanine (D-Phe) imprinted polymeric beads and increase the adsorption capacity and selectivity. They prepared the D-Phe-imprinted beads with a minimum size of 2.38  $\mu$ m [16]. The further decrease in beads size using the modified suspension polymerization was not successful because of the generation of unfavorable conditions for radical safety at high rotation speed. The basic reason was the entrapment of atmospheric oxygen at higher rotation speed, which acts as radical scavenger and reacts with free radicals and

<sup>†</sup>To whom correspondence should be addressed.  
E-mail: parkjk@knu.ac.kr

hinders the polymerization process. Considering the importance of nanosized MIPs compared to microbeads, the use of cost-effective modified suspension polymerization would be of great value if it could be used for the production of submicron/nanosized beads. For this purpose, the prevention of oxygen entrapment in the polymerization mixture at high rotation speed was adopted using the continuous supply of inert gas. The technique was modified by arranging a system employing continuous supply of  $N_2$  during polymerization. This technique provided favorable conditions for radical safety during polymerization even at higher rotation speed and, as a result, Phe-imprinted submicron/nanoscale beads with the improved adsorption capacity and selectivity were obtained successfully for the first time. In this study, the L-Phe-imprinted, D-Phe-submicron/nanoscale imprinted and non-imprinted beads were also prepared and a comparative study was done. Furthermore, the effect of template on the size distribution and the performance of the prepared submicron/nanoscale beads was correlated by FE-SEM, FT-IR and  $^{13}C$  CP-MAS NMR spectroscopy. The effect of racemate solution concentration was also studied and the prepared beads were used for five successive batch experiments.

## MATERIALS AND METHODS

### 1. Materials

D-Phe, L-Phe, D,L-Phenylalanine racemic mixture (Phe), methacrylic acid (MAA), ethyleneglycoldimethacrylate (EGDMA), and trifluoroacetic acid (TFA) were purchased from Sigma-Aldrich (St Louis, MO, USA); 2,2-azobisisobutyronitrile (AIBN) was obtained from Junsei Chemical Co., Ltd. (Japan); toluene was the product of Duksun Pure Chemical Co., (Korea); SDS was from Fluka (Switzerland), polyvinyl alcohol (PVA) and copper sulfate ( $CuSO_4 \cdot 5H_2O$ ) were obtained from Yakuri Pure Chemicals Co., (Osaka, Japan). All reagents used were of analytical reagent grade.

### 2. Preparation of Submicron/Nanoscale Beads

For preparing D-Phe- and L-Phe-imprinted submicron/nanoscale beads, initially four types of solutions were prepared as described in previous studies [3,16,19].

**Solution-1:** D-Phe or L-Phe (0.116 g, 1 mmol), MAA (0.34 mL, 4 mmol), toluene (3 mL), acetic acid (0.6 mL), TFA (0.4 mL) were taken in a 10 mL vial and all the components were dissolved by stirring the solution for 10 min at room temperature. Then, in the next step the solution was stirred at  $0^\circ C$  for 30 min.

**Solution-2:** EGDMA (3.77 mL, 20 mmol), toluene (2 mL) and AIBN (0.15 g) were taken in a 50 mL flat bottom flask and stirred for 10 min at room temperature.

**Solution-3:** PVA (3.45 g) was dissolved in distilled water (130 mL) by stirring in a 250 mL flask for 30 min at  $80-85^\circ C$  and then cooled at room temperature.

**Solution-4:** SDS (1 g) was dissolved in water (20 mL) by stirring in a 250 mL flask for 20 min at room temperature.

After this, solution-1 and solution-2 as well as solution-3 and solution-4 were combined together separately. These solutions were stirred separately for 2 h and then mixed in a three-necked double jacket glass vessel, purged with  $N_2$  for 5 min, and stirred at 650 rpm for 60 min at room temperature. Polymerization was carried out at  $60^\circ C$  for 24 h under  $N_2$  atmosphere by supplying continuously  $N_2$  gas through a needle into the vessel at a low pressure of about 1

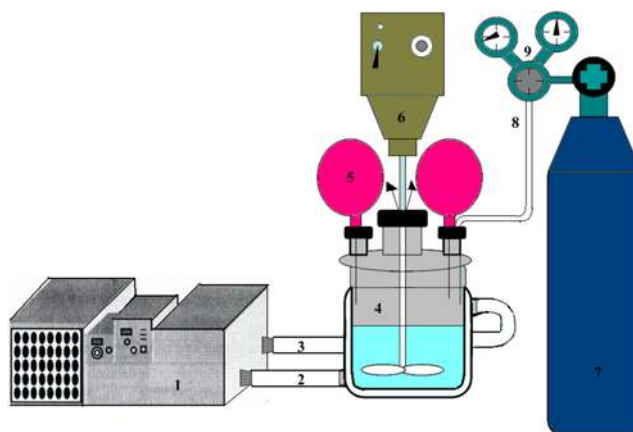


**Fig. 1. Schematic diagram of modified suspension polymerization process used for the preparation of submicron/nanoscale beads.**

- |                                  |                              |
|----------------------------------|------------------------------|
| 1. Shaking bath circulator       | 6. Stirrer machine           |
| 2. Water into the reactor vessel | 7. $N_2$ gas cylinder        |
| 3. Water out from reactor vessel | 8. $N_2$ into reactor vessel |
| 4. Reactor vessel                | 9. Barometers                |
| 5. Balloon                       |                              |

pound-force/inch<sup>2</sup> (psi), and with continuous stirring at 650 rpm. This polymerization process resulted in submicron/nanosized beads. The schematic representation of the abovementioned modified suspension polymerization process is represented as Fig. 1.

### 3. Washing of the Prepared Beads

To remove the unreacted chemicals the prepared MIP beads L-Phe imprinted submicron/nanoscale beads (LIBs), D-Phe imprinted submicron/nanoscale beads (DIBs) and non-imprinted nanoscale beads (NIBs) were washed initially with 5% (v/v) ethanol followed by washing with distilled water. After this LIBs and DIBs were washed with 5% (v/v) acetic acid solution for 3 h followed by washing with distilled water for 1 h. These alternative washings with 5% acetic acid and distilled water were repeated up to eight times until complete removal of template molecules. For conducting an effective washing during each washing step, ultrasonication was done for 3 to 5 min. The residual acetic acid was removed from the beads matrix with an excess of distilled water until the pH of the aqueous solution increased to the pH of distilled water.

### 4. FE-SEM Analysis

Scanning electron microscopy (SEM) of the freeze-dried LIBs, DIBs and NIBs was performed using a Hitachi S-4800 & EDX-350 (Horiba) FE-SEM (Tokyo Japan). Samples were fixed on the brass holder and coated with  $OsO_4$  by VD HPC-ISW osmium coater (Tokyo Japan) prior to FE-SEM observation. FE-SEM analysis was also used for determining the beads size distribution.

### 5. Fourier Transform Infrared Spectroscopy (FT-IR)

Infrared spectra of the dried nanobeads were recorded with an FTIR spectrophotometer (spectrum GX Autoimage). The spectral range for the analysis was  $400-5,000\text{ cm}^{-1}$ . Beam splitter: Ge coated on KBr - detector DTGS - Resolution:  $0.25\text{ cm}^{-1}$  (step selectable). For analysis the dried beads were mixed with KBr in the ratio of 1 : 100 and the spectra were recorded.

### 6. $^{13}C$ CP-MAS NMR Spectroscopy

Solid state  $^{13}C$  CP-MAS NMR study was conducted with Unity

INOVA (Varian., USA) using solid state  $^{13}\text{C}$  NMR at 600 MHz (14.1T). The spectral range was 400--50 ppm.

### 7. Batch Experiments

The imprinted submicron/nanoscale beads (0.1 g) were added to 2 mL of 100 mg  $\text{L}^{-1}$  of Phe racemate solution and shaken for 7 h at 25 °C and 150 rpm. After adsorption, the sample was centrifuged at 13,000 rpm for 3 min and filtered through Whatman® PVDF syringe filter (0.45  $\mu\text{m}$ ). The filtered samples were then analyzed with HPLC. Same procedure was followed for batch adsorption with non-imprinted beads.

The effect of pH on the adsorption capacity and selectivity of LIBs, DIBs and NIBs was investigated at pH 2, 4 and 6 at 25 °C. Equilibrium adsorption time was determined by conducting batch adsorption from 1 to 24 h at 25 °C and 150 rpm. For studying the concentration effect, Phe solution in the concentration range of 25 mg  $\text{L}^{-1}$  to 1,000 mg  $\text{L}^{-1}$  was prepared and used in batch adsorption experiments. All the experiments were repeated in triplicate.

### 8. HPLC Analysis

The amounts of D-Phe and L-Phe in the obtained samples were determined with HPLC equipped with an M930 solvent delivery pump and M720 UV absorbance detector (Young-Lin Instruments, Anyang, Korea). A TSK gel Enantio L2 column (Tosoh, Tokyo, Japan) with dimensions of 4.6 mm  $\times$  250 mm was used.

From HPLC results the adsorbed amount of enantiomers and adsorption selectivity of the prepared LIBs, DIBs and NIBs were calculated by the following equations [20].

### 9. Amount of Phe Adsorbed

$$Q = (C_i - C_e) \times V / W \quad (1)$$

Where Q is the amount of D- or L-Phe adsorbed on the beads (mg  $\text{g}^{-1}$ ), while  $C_i$  and  $C_e$  are the initial concentration (mg  $\text{L}^{-1}$ ) in feed solution and concentration (mg  $\text{L}^{-1}$ ) after adsorption, respectively. V is the volume in liter and W is the dry weight in grams.

### 10. Adsorption Selectivity

$$\alpha_{\text{ads}} = \frac{\{(Q_1)/(Q_2)\}}{\{[\text{Template}]/[\text{Counter enantiomer}]\}} \quad (2)$$

Where  $\alpha_{\text{ads}}$  is the adsorption selectivity, ( $Q_1$ ) and ( $Q_2$ ) are the amounts (mg) of template and the counter enantiomer adsorbed per 1 g of dry beads, respectively, and  $[\text{Template}]/[\text{Counter enantiomer}]$  is the ratio of concentration (mg  $\text{L}^{-1}$ ) of template and counter enantiomer.

## RESULTS AND DISCUSSION

### 1. Extraction of Template Molecules from the Polymer Matrix of LIBs and DIBs

Proper washout of template from the imprinted polymer matrix is an important step because it makes the binding sites available and also controls the bleeding from the MIP beads [20,21]. In this study, 5% (v/v) acetic acid solution was used along with employing ultrasonication for efficient extraction of template (L- or D-Phe) molecules from the submicron/nanoscale beads. 5% (v/v) acetic acid solution was also used previously for desorption of template molecules [16,19]. The data for overall template extraction shown in Fig. 2 indicates that most of the template molecules (more than 80%), were washed out during initial five alternative washings with acetic acid solution and distilled water. However, after the fifth wash-

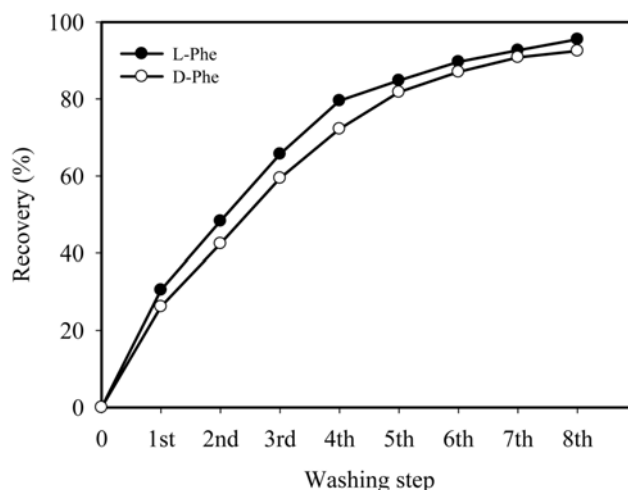


**Fig. 2.** Amount of L- and D-Phe recovered from LIBs and DIBs, respectively. First washing was done with 5% (v/v) ethanol and distilled water for 1 h each followed by washing with 5.0% (v/v) acetic solution and distilled water for 3 and 1 h, respectively. All other washings were done with 5.0% (v/v) acetic acid solution for 3 h followed by 1 h washing with distilled water. The washing was conducted on the orbital shaker at 150 rpm and 25 °C.

ing still the washing was required until the eighth wash with acetic acid solution, followed by distilled water to completely remove the template molecules (when no template molecule was observed) from the polymer matrix. It was found that 95.5 and 92.5% of L- and D-Phe, respectively, were removed after complete washing of LIBs and DIBs, respectively. The effective desorption was caused by the smaller size of the submicron/nanoscale beads. The purpose of applying ultrasonication during washing was to help in extraction of the template molecules situated deeply inside the beads [20,21] and to resolve and overcome any agglomerates of the submicron/nanosized beads.

### 2. FE-SEM Study

The particle shape, size, and porosity are considered important because these parameters control the specific surface area, mass transfer rate as well as the adsorption properties of the prepared MIP beads [22,23]. From the SEM micrographs shown in Fig. 3(a)-(f) it is clear that in all types of beads (LIBs, DIBs and NIBs) the size is in the submicron to nanoscale, i.e., 1.5  $\mu\text{m}$  to 100 nm. Similarly, Fig. 3(b), (d) and (f) show the surface morphology of the beads at higher magnification. All types of beads are spherical with rough surfaces. Fig. 4 indicates that the content of nanosized beads in LIBs and DIBs was more than 65%, while in the case of NIBs all the beads were in nano level. The smaller size of NIBs compared to MIP beads was also observed previously [18]. The reason for this difference in size was the presence of template molecules during the formation of the MIP bead polymerization process [18,24]. The presence of template molecules might have affected the polymerization process, which in turn caused the difference in sizes of the prepared imprinted (LIBs, DIBs) and NIBs. In the present study it was found that the template type also affects the beads size, as is clear from Fig. 3 and Fig. 4 which show that average size of the LIBs was slightly larger than that of DIBs. These facts are proved from the  $^{13}\text{C}$  CP-

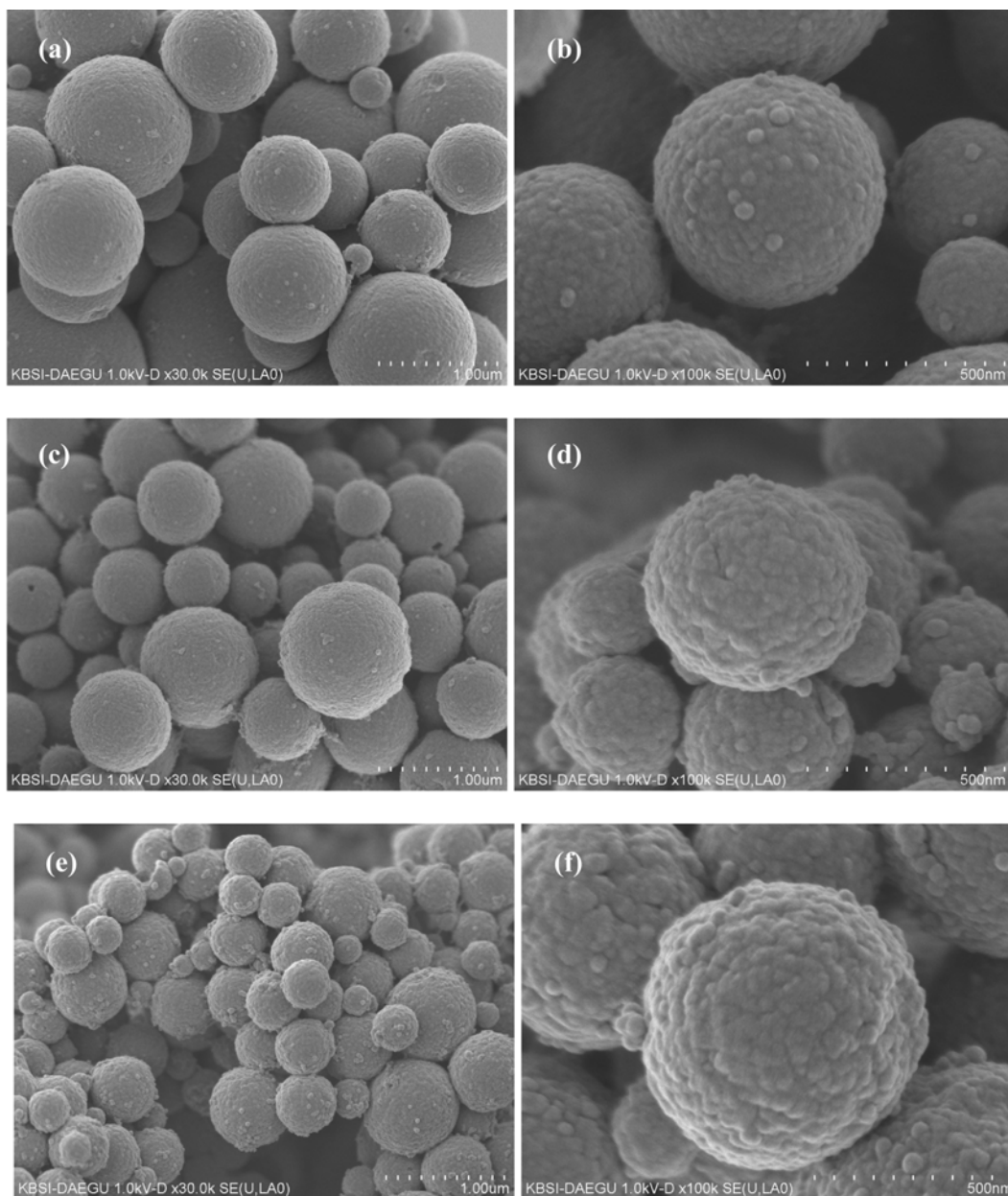


**Fig. 3.** FE-SEM micrographs of submicron/nanoscale MIP and NIP beads prepared by modified suspension polymerization, where (a) LIBs (1.0 kV-D x 30.0k), (b) LIBs (1.0 kV-D x 100k), (c) DIBs (1.0 kV-D x 30.0k), (d) DIBs (1.0 kV-D x 100k), and (e) NIBs (1.0 kV-D x 30.0k), (f) NIBs (1.0 kV-D x 100k).

MAS NMR study, which is explained in the following section in detail. Besides, in the present case the size range is smaller than the previously reported microbeads where the lowest mean particle size of 2.38  $\mu\text{m}$  and 8.90  $\mu\text{m}$  was observed [16,19]. The main cause for this decrease in size was the use of high rotation speed in the presence of surfactant (SDS) and stabilizer (PVA), which resulted in much smaller beads compared to previous studies [16,19]. The use of high rotation speed could produce the chances of  $\text{O}_2$  entrapment during polymerization. Hence, in the present study the continuous supply of  $\text{N}_2$  at low pressure was made to overcome the entrapment of  $\text{O}_2$  at high rotation speed (Fig. 1). Thus, the steady continuous supply of  $\text{N}_2$  resulted in effective polymerization to produce submicron/nanoscale beads. Furthermore, it is already known that micelles are

much smaller than suspension droplets [16]. The increase in rotation speed might have caused a reduction in micelle size, which resulted in the smaller bead size. Hence, this study proves that while employing modified suspension polymerization method the use of high rotation speed resulted in the production of much smaller, i.e., submicron to nanosized, beads. All types of the prepared beads also maintained the spherical shapes with rough and porous surfaces compared to previously prepared MIP nanoscale particles/beads [9,18,25], where in most of cases a high degree of agglomeration was found and mostly the particles were also not with proper spherical shapes. Hence, the spherical shapes and suitable sizes of the presently prepared submicron/nanoscale beads are beneficial for high adsorption affinity, which makes these beads suitable to be used in

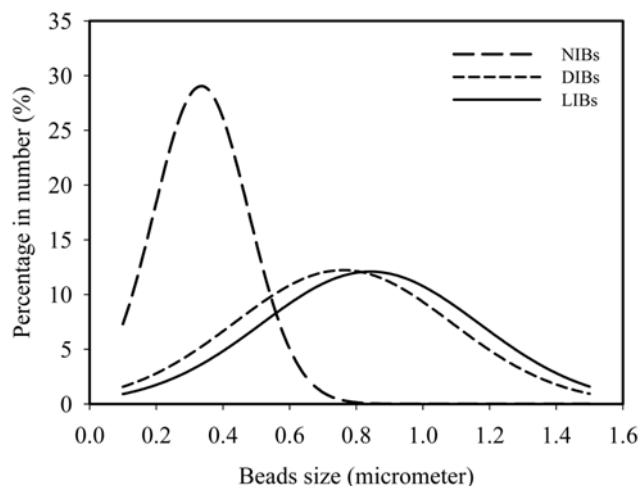


**Fig. 4.** Size distribution of LIBs, DIBs and NIBs determined from FE-SEM analyses.

several different applications. Moreover, this study clarified that the presence and type of template molecules had an evident effect on the mean particle sizes of the prepared beads.

### 3. FT-IR and $^{13}\text{C}$ CP-MAS NMR Spectroscopy for Structural Characterization

For measuring the degree of polymerization and reactivity for each type of polymerizable group on the monomer within the polymer, FT-IR and  $^{13}\text{C}$  CP-MAS NMR are considered as useful tools [26]. The chemical structures and functionalities of the LIBs, DIBs and NIBs were determined by FT-IR and  $^{13}\text{C}$  CP-MAS NMR spectroscopy. The FT-IR spectra of the prepared beads are given in Fig. 5 in which the peak at  $3,446\text{ cm}^{-1}$  represents OH stretching of free carboxylic group derived from MAA (functional monomer), while the peak at  $1,734$ ,  $1,638$  and  $2,996$  and  $2,962\text{ cm}^{-1}$  stand for  $\text{C}=\text{O}$ ,  $\text{C}=\text{C}$ , and  $\text{CH}$  stretching, respectively. The peaks at  $1,264$  and  $1,163\text{ cm}^{-1}$  were assigned to the  $\text{CO}$  bending of ester group and  $\text{CO}$  stretching of  $\text{COOH}$  and ester groups. The small absorption bands at  $951$ ,  $806$ , and  $753\text{ cm}^{-1}$  were attributed to  $\text{C}-\text{CH}_3$  rocking,  $\text{CH}$  bending

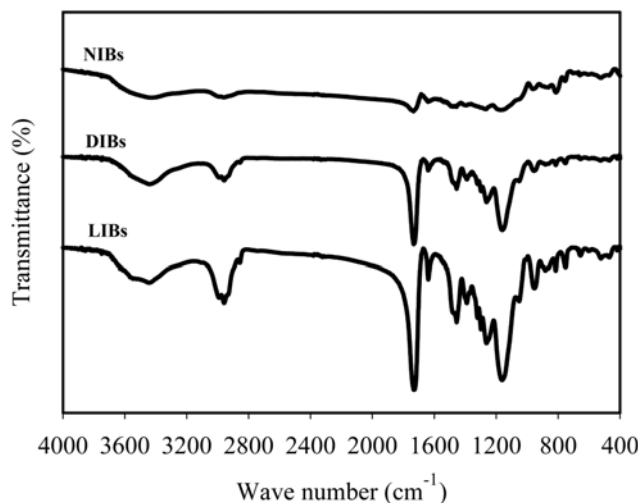


**Fig. 5.** FT-IR spectra of LIBs, DIBs and NIBs prepared by modified suspension polymerization.

(vinyl out of plane), and  $\text{CH}_2$  rocking, respectively. Similar results were also obtained in previously reported studies [2,16] related to the imprinted Poly(MAA-co-EGDMA) polymers. However, compared to FT-IR spectrum of D-Phe microbeads [16], three new peaks at  $1,295$ ,  $1,326$  and  $2,842\text{ cm}^{-1}$  also appeared, which correspond to the stretching of  $\text{CO}$  of  $\text{COOH}$ , deforming of  $\text{OH}$  of carboxylic group and symmetric stretching of  $-\text{CH}_2$ , respectively [27]. From these spectra, it is clear that the hydroxyl peak at  $3,445\text{ cm}^{-1}$  for LIBs and DIBs is stronger than that for NIBs. Similarly, the intensities of other absorption peaks at  $1,734$ ,  $1,264$  and  $1,163\text{ cm}^{-1}$  which correspond to  $\text{C}=\text{O}$  and  $\text{CO}$  groups, respectively, were also found to be higher in case of LIBs and DIBs compared to NIBs. This indirectly confirms the formation of recognition sites in the LIBs and DIBs because of the existence of a large population of free carboxyl groups after template removal [2,16,27]. Additionally, the appearance of new peaks at  $1,326\text{ cm}^{-1}$  for  $\text{OH}$  deformation and at  $1,295$  for  $\text{CO}$  stretching also confirms the presence of higher number of these groups in the submicron/nanoscale beads prepared in the present study. This in turn indicates the higher number of binding sites in the submicron/nanoscale beads compared to previously reported microbeads [16].

The  $^{13}\text{C}$  CP-MAS NMR spectra of the LIBs, DIBs and NIBs are given in Fig. 6. The two distinct peaks at  $177$  and  $167\text{ ppm}$  were observed and assigned to carbonyl carbon of free  $\text{COOH}$  group derived from MAA and acetyl group derived from EGDMA (cross linker), respectively [26,28,29]. The other peaks at  $61$ ,  $46$  and  $19\text{ ppm}$  were attributed to  $\text{CH}_2$  of the ester group,  $-\text{CH}_2-$  quaternary carbons and methyl groups of main aliphatic carbon chain, respectively [29]. The two small peaks at  $137$  and  $124\text{ ppm}$  were due to the vinyl carbon of the unreacted monomers. It was found that in the present study the peaks at  $177$ ,  $61$  and  $124\text{ ppm}$  appeared slightly upfield compared to  $178$ ,  $63$  and  $127\text{ ppm}$  in the  $^{13}\text{C}$  CP-MAS NMR spectrum for previously prepared microbeads [16]; (spectrum not shown). This slight upfield shift indicates that the reduction in bead sizes to submicron/nanoscale also resulted in a slight increased shielding of the carbon of the abovementioned groups. This change may be due to the higher number of free  $\text{OH}$  and  $\text{C}=\text{O}$  groups where

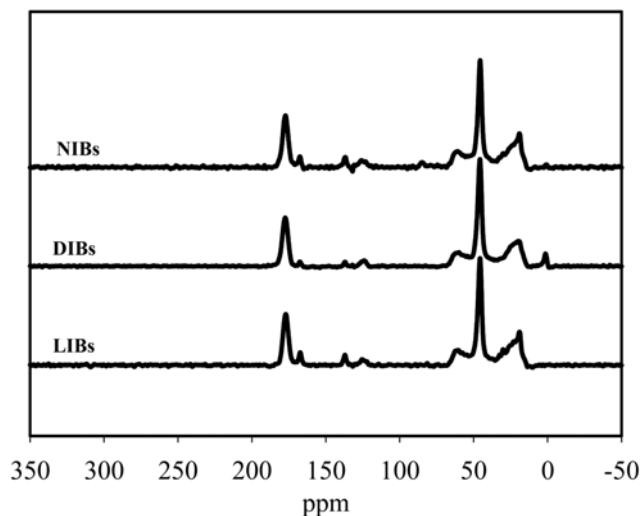


**Fig. 6.**  $^{13}\text{C}$  CP-MAS NMR spectra of LIBs, DIBs and NIBs prepared by modified suspension polymerization.

high density of  $\pi$  bonded and free electrons caused the shielding of these carbon atoms.

The purpose of  $^{13}\text{C}$  CP-MAS NMR study was also to elucidate the content of saturated and unsaturated bonds and further elaboration of the polymer structure [26,28,29]. Following the reported method [26,29] the intensity of peaks at 177 and 167 ppm was determined to determine the extent of CO group attached to the saturated (-C-C-) and unsaturated groups (-C=C-) [26,28,29], respectively. In all types of beads (LIBs, DIBs and NIBs) the content of saturated bonds was in the range of 84-90%, which is in agreement with the reported study [29]. The LIBs had the lowest content of unsaturated bonds (C=C) 10.20% followed by 11.04 and 14.29% in case of DIBs and NIBs, respectively. It indicates that the extent of polymerization in LIBs was 89.80% followed by 88.97 and 85.71% in case of DIBs and NIBs, respectively [28,29]. Similarly, this is also an indication of high reaction rate in MIP bead formation compared to NIBs [28,29]. From this study it may be said that the relatively high extent of reaction in MIP beads might be due to the presence of template molecules during polymerization. The template molecules might have affected the double bonds of EGDMA and MMA during polymerization by steric effect and made it more suitable for polymerization. However, this needs further investigation. In LIBs and DIBs the higher sum of C=O bonds attached to the saturated -C-C- bond indirectly supports the presence of high number of binding sites formed after removal of template molecules.

This whole structural characterization supported the fact that all

types of the prepared submicron/nanoscale beads had maintained the basic structural features of P (MAA-co-EGDMA). In addition, this study also proved the presence of basic structural characteristics of imprinted polymers which are of prime importance.

#### 4. Adsorption Capacity and Selectivity of the Prepared Submicron/Nanoscale Beads

The adsorption capacity and selectivity are the basic parameters which determine the utility of molecularly imprinted polymers. It is already known that the bead size has an evident effect on the performance of molecularly imprinted polymers [10-12]. In the present study the prepared submicron/nanoscale beads were used for resolution of Phe racemate solution, and its adsorption capacity and selectivity were determined and compared to the previously reported results.

A comparative study of adsorption selectivity of the presently prepared submicron/nanoscale beads and the previously reported MIP beads used in batch adsorption is indicated in Table 1. It is evident from Table 1 that compared to other types of MIP beads used in batch adsorption [2,16,19,30-34] the presently prepared submicron/nanoscale beads showed higher or almost comparable [35,36] adsorption selectivity. However, the overall comparative study points out that the reduction in size to submicron/nanoscale has greatly improved the selectivity property of the prepared beads. Likewise, the adsorption capacity of these beads shown in Table 2 was also higher compared to the previously reported microbeads prepared by suspension polymerization [16]. In present case an increase in

**Table 1. Comparison of size and adsorption selectivity (during batch adsorption) of submicron/nanoscale beads (LIBs, DIBs and NIBs) obtained in the present study with size and adsorption selectivity (during batch adsorption) of beads reported in literature**

Polymerization method	Template	Beads size	Adsorption selectivity	Reference
Modified suspension <sup>a</sup>	L-Phe	0.1-1.5 $\mu\text{m}$	1.62	Present
	D-Phe	0.1-1.5 $\mu\text{m}$	1.59	
	Non-imprinted	0.1-0.8 $\mu\text{m}$	1.02	
Modified suspension <sup>a</sup>	D-Phe	2.38 $\mu\text{m}$	1.32	[16]
Modified suspension <sup>a</sup>	D-Phe	12.5 $\mu\text{m}$	1.28	[19]
Suspension	Tyrosine	60-255 $\mu\text{m}$	1.91	[36]
Suspension	S-propranolol	50-65 $\mu\text{m}$	1.60	[31]
Sol-gel transition	D-Phe	2.0-4.4 mm	1.33	[2]
In situ polymerization	D-Phe	-	0.81	[27]
Bulk	L-PheAN	1.0-15 $\mu\text{m}$	1.65	[35]
Bulk	D- or L-Phe	10-50 $\mu\text{m}$	1.47	[32]
Bulk	D-Phe	mm range	1.38	[33]
Bulk	Sulfur mustard	-	1.30	[34]

<sup>a</sup>Modified suspension polymerization method using turbine impeller

**Table 2. Adsorption capacity and selectivity of submicron/nanoscale beads (LIBs, DIBs and NIBs) prepared by modified suspension polymerization method at a stirring speed of 650 rpm. Conditions: 0.1 g of dried beads; Phe racemate solution concentration: 100 mg L<sup>-1</sup>; volume: 2 mL; adsorption time: 7 h; temperature: 25 °C; shaking speed: 150 rpm**

Beads	pH 2		pH 4		pH 6	
	Adsorption capacity (mg/g)	Adsorption selectivity	Adsorption capacity (mg/g)	Adsorption selectivity	Adsorption capacity (mg/g)	Adsorption selectivity
LIBs	0.351	1.624	0.301	1.467	0.331	1.588
DIBs	0.300	1.587	0.276	1.443	0.284	1.565
NIBs	0.186	1.023	0.173	1.012	0.186	1.024

selectivity is certainly due to reduction in size of the beads. Bompert and Haupt mention that the nanoscale MIPs have several advantages such as high surface to volume ratio, short diffusion distance, homogeneous site distribution and regular shape and sizes [14]. All these properties improve the mass transfer and binding kinetics, which in turn results in high adsorption capacity and selectivity of the MIP system [9,31]. Hence, the present improved results also agree with these facts. Furthermore, the FT-IR (Fig. 5) and  $^{13}\text{C}$  CP-MAS NMR spectra (Fig. 6) also support the mentioned reasons responsible for the improved adsorption capacity and selectivity of the prepared submicron/nanoscale beads. Moreover, the improvement in adsorption capacity and selectivity is due to almost complete washing of the template from the prepared beads as well as to smaller beads sizes, which caused the easy excess of molecules to the available functional sites.

### 5. Effect of pH and Template

The pH condition for adsorption experiments was optimized. Table 2 shows that the adsorption capacity and selectivity of the prepared submicron/nanoscale beads was higher at pH 2 compared to pH 4 and 6. It is clear from Table 2 that at pH 2 the total adsorption amount of D-Phe and L-Phe is 0.35, 0.30 and 0.19  $\text{mg g}^{-1}$  for LIBs, DIBs and NIBs, respectively. Similarly, it also indicates that at pH 2 the maximum selectivity of LIBs, DIBs and NIBs was 1.62, 1.59 and 1.02, respectively. Park et al. [5] and Chen et al. [37] reported the high adsorption capacity and selectivity of template was obtained at lower pH rather than at higher pH. According to them, the basic reason for the higher adsorption capacity and selectivity at acidic conditions was the presence of higher number of COOH groups in the polymer matrix as well as on the template. However, Khan and Park [16] further evaluated the effect of pH by considering the role of  $\text{NH}_3^+$  and  $\text{COO}^-$  in the imprinting process through ionic interaction along with hydrogen bonding by COOH groups. Hence, in the present study, the better results at pH 2 are due to the presence of high content of effective functional groups (COOH) in the polymer matrix as well as template molecules in the racemate solution at pH 2 compared to pH 4 and 6. On the other hand, slightly better results at pH 6 compared to pH 4 are due to the ionic interactions caused by  $\text{NH}_3^+$  of template and  $\text{COO}^-$  of polymer matrix in addition to hydrogen bonding [16]. In the present study, the relatively higher adsorption capacity and selectivity of LIBs compared to DIBs might be due to the presence of higher number of functional sites on the LIBs compared to DIBs. This fact is clear from FT-IR spectra (Fig. 5). Similarly,  $^{13}\text{C}$  CP-MAS NMR study shown in Fig. 6 also supports slightly better structural characteristics of LIBs compared to DIBs. In addition, relatively higher extraction of template from LIBs compared to DIBs may be considered a reason for comparatively better results in the case of LIBs. However, this needs further investigation.

Studies were made to analyze the effect of template on adsorption capacity and selectivity. In this regard, contrary to our previous studies [3,16,19], the LIBs, DIBs and NIBs were prepared and their comparative study was performed. Table 2 and all other results illustrate that the imprinted beads showed much better results than non-imprinted beads. It is clear from Table 2 that the adsorption capacity and adsorption selectivity of LIBs was slightly higher compared to DIBs, which is in agreement with previous results obtained for MIP membranes [38]. The higher adsorption selectivity of LIBs

may be explained in terms of a higher extraction of template from LIBs compared to DIBs as clear from the washing study given in Fig. 2. The FTIR (Fig. 4) and  $^{13}\text{C}$  CP-MAS NMR (Fig. 6) also support the higher adsorption capacity and selectivity of LIBs compared to DIBs and NIBs.

### 6. Effect of Racemate Concentration

The amount of substances adsorbed is determined as a function of the racemate concentration at constant temperature. The effect of concentration on adsorption capacity and selectivity was determined at 25 °C. Fig. 7(a), (b), and (c) indicate that the increase in

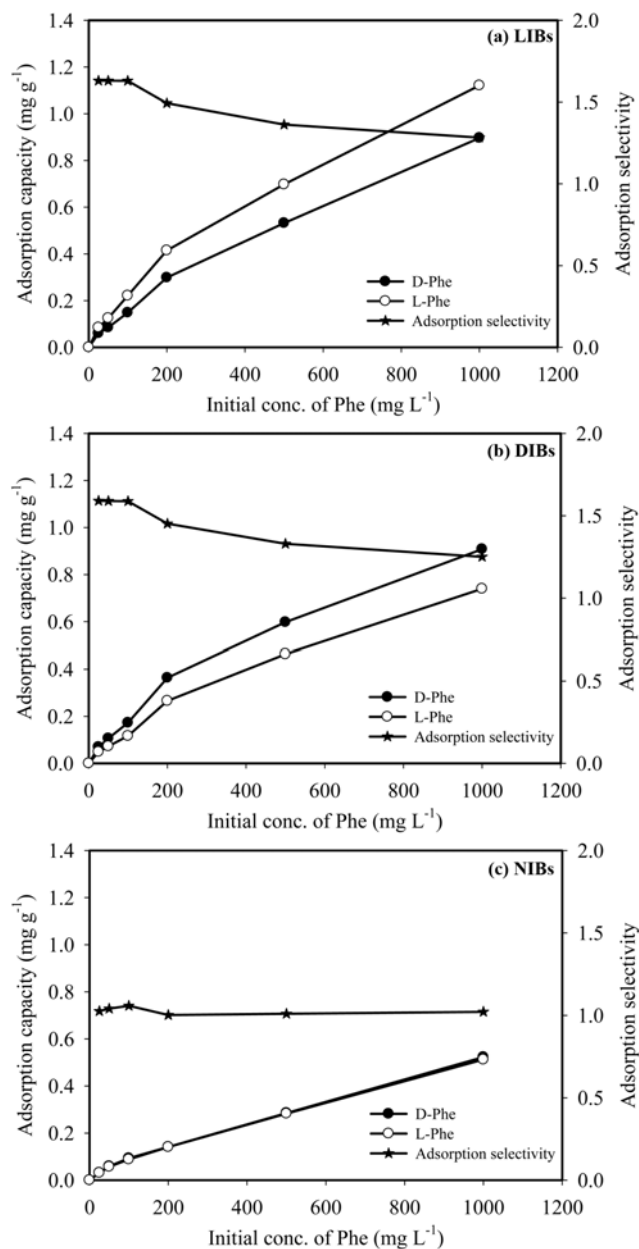


**Fig. 7.** Adsorption capacity and selectivity profile of D- and L-Phe onto (a) LIBs, (b) DIBs and (c) NIBs, prepared by modified suspension polymerization method at a stirring speed of 650 rpm. The adsorption experiments were performed for 7 h using 0.1 g of dried beads and 2 mL of different concentrations of Phe racemate solution (25 to 1,000  $\text{mg L}^{-1}$ ) at 25 °C and 150 rpm.



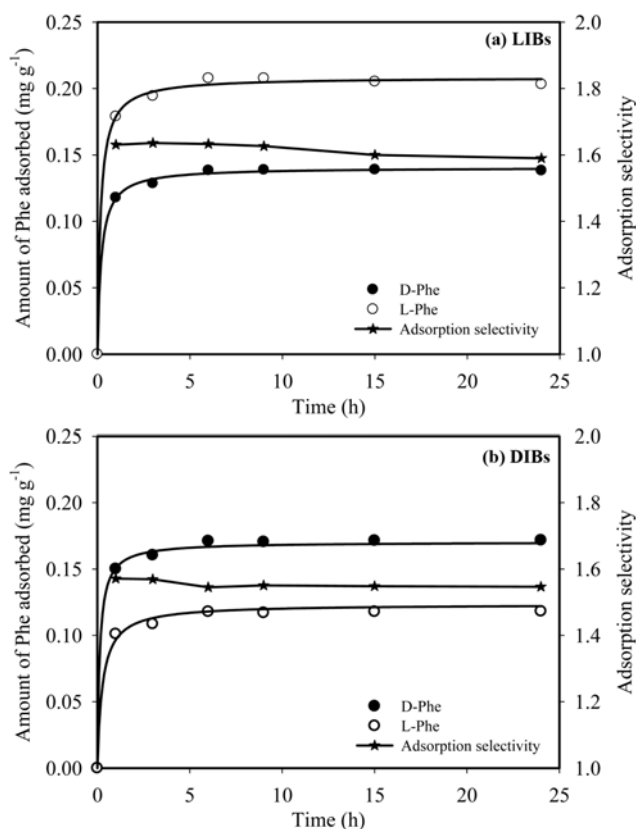


**Fig. 8.** Adsorption profiles of D- and L-Phe where (a) LIBs and (b) DIBs prepared by modified suspension polymerization method. The adsorption experiments were performed for different interval of time (1 to 24 h) using 0.1 g of dried beads and 2 mL of 100 mg L<sup>-1</sup> Phe racemate solution at 25 °C and 150 rpm.

concentration of Phe racemate solution had an evident effect on the adsorption capacity and selectivity of the prepared submicron/nanoscale beads. Fig. 7(a) and (b) indicate that with increase in initial concentration of Phe racemate solution the adsorption capacity of LIBs and DIBs increased to a higher extent compared to NIBs Fig. 7(c). It is also clear from Fig. 7(a) and (b) that with increase in concentration of Phe the adsorption selectivity of LIBs and DIBs was reduced. The maximum adsorption selectivity was observed up to 100 mg L<sup>-1</sup> of Phe racemate solution, and beyond that the adsorption selectivity was reduced. This was because with increase in concentration of the racemate solution the non-specific adsorption was increased, which resulted in higher adsorption capacity and lower adsorption selectivity of LIBs and DIBs. However, the overall adsorption capacity and selectivity of the presently prepared submicron/nanoscale beads was higher than the microbeads [16] even after the fifth batch.

### 7. Equilibrium Adsorption Time

The time dependence of Phe adsorption onto LIBs and DIBs from aqueous solution was determined in batch adsorption experiments. Fig. 8(a) and (b) indicate the adsorption equilibrium curve of LIBs and DIBs respectively. It was found that the adsorption rate of Phe was higher initially and then slowed down when approaching equilibrium. The adsorption equilibrium for LIBs and DIBs was achieved within 6 h. More than 90% of equilibrium amount was adsorbed

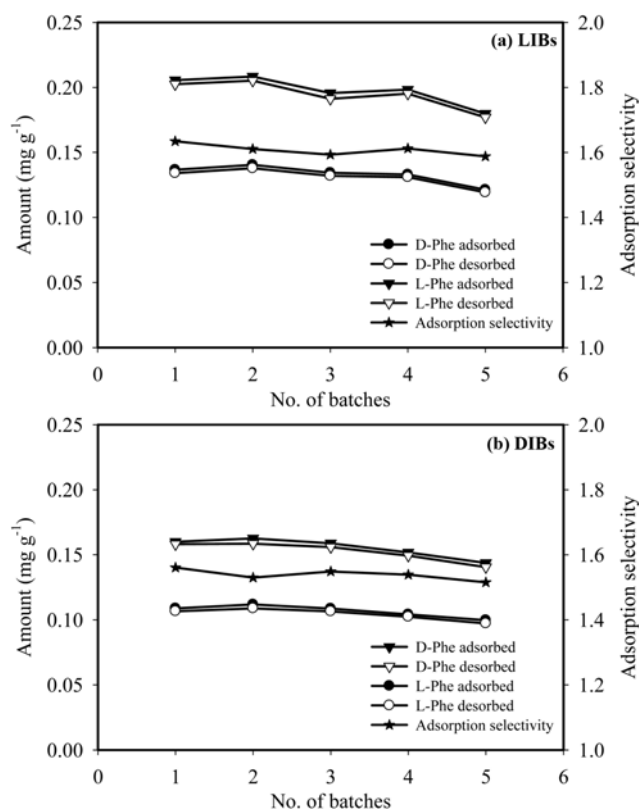


**Fig. 9.** Adsorption and desorption profiles of D- and L-Phe where (a) LIBs and (b) DIBs prepared by modified suspension polymerization method.

within initial 3 h for D- and L-Phe. It is also evident from Fig. 8(a) and (b) that the adsorption selectivity remained almost the same throughout the course of experiment. A comparative study of the adsorption equilibrium curves for LIBs (Fig. 8(a)) and DIBs (Fig. 8(b)) showed that the adsorption equilibrium was achieved within the same interval of time. This was due to fact that both have almost similar bead sizes.

### 8. Desorption and Reusability

Sufficient economic improvement can be brought about by increasing the regenerative efficiency of the adsorbents. The adsorbed amount of Phe was recovered by extraction with 5% (v/v) acetic acid and distilled water. Adsorption and desorption experiments were performed till five successive batches to confirm the reusability of LIBs and DIBs. More than 98% of adsorbed amount of template was desorbed in each desorption experiment. It is clear from Fig. 9(a) and (b) that successive batch adsorption and desorption did not affect the adsorption capacity and selectivity of the prepared MIP submicron/nanoscale beads. Fig. 9(a) and (b) clearly show that the adsorption capacity and selectivity of both D- and L-Phe remained almost constant until the fifth batch. The reusability of the LIBs and DIBs greatly influences the economic feasibility of the modified suspension polymerization process and the use of submicron/nanoscale beads in the imprinting process.

## CONCLUSIONS

Submicron/nanoscale MIP beads with higher adsorption capac-



ity and selectivity were prepared by modified suspension polymerization at higher rotation speed under continuous N<sub>2</sub> supply. Washing of the prepared MIP beads (LIBs and DIBs) with 5% acetic acid solution along with using sonication process resulted in effective extraction (more than 92%) of template molecules from the polymer matrix. The template has an evident effect on the bead size, and the pH controls the extent of effective functional sites on the polymer matrix. LIBs and DIBs maintained their higher adsorption capacity and selectivity till five consecutive batches. The prepared submicron/nanoscale beads have regular spherical shapes with rough and porous surfaces and very low agglomeration. FT-IR and <sup>13</sup>C CP-MAS NMR studies supported the presence of higher content of functional sites as well as the larger sizes of the prepared MIP beads than that of NIBs. From this whole study it was inferred that due to smaller sizes, regular shapes and high adsorption and separation properties, the prepared MIP submicron/nanoscale beads can be used for several applications such as separation, purification, analysis and detection.

## REFERENCES

1. M. Komiyama, T. Takeuchi, T. Mukawa and H. Asanuma, *Molecular imprinting from fundamentals to applications*, ©WILEY-VCH GmbH and Co. KGaA Weinheim, ISBN 3-527-30569-6 (2003).
2. J. K. Park, H. Khan and J. W. Lee, *Enzym. Microb. Technol.*, **35**, 688 (2004).
3. H. Khan, T. Khan and J. K. Park, *Sep. Purif. Technol.*, **62**, 363 (2008).
4. H. H. Yang, S. Q. Zhang, F. Tan, Z. X. Zhuang and X. R. Wang, *J. Am. Chem. Soc.*, **127**, 1378 (2005).
5. J. K. Park, S. J. Kim and J. W. Lee, *Korean J. Chem. Eng.*, **20**, 1066 (2003).
6. P. Fan and B. Wang, *Korean J. Chem. Eng.*, **26**, 1813 (2009).
7. Y. Jin, D. K. Choi and K. H. Row, *Korean J. Chem. Eng.*, **25**, 816 (2008).
8. I. Surugiu, B. Danielsson, L. Ye, K. Mosbach and K. Haupt, *Anal. Chem.*, **73**, 487 (2001).
9. Y. Li, X. F. Yin, F. R. Chen, H. H. Yang, Z. X. Zhuang and X. R. Wang, *Macromolecules*, **39**, 4497 (2006).
10. M. A. Markowitz, P. R. Kust, G. Deng, P. E. Schoen, J. S. Dordick, D. S. Clark and B. P. Gaber, *Langmuir*, **16**, 1759 (2000).
11. D. Gao, Z. Zhang, M. Wu, C. Xie, G. Guan and D. Wang, *J. Am. Chem. Soc.*, **129**, 7859 (2007).
12. C. Xie, B. Liu, Z. Wang, D. Gao, G. Guan and Z. Zhang, *Anal. Chem.*, **80**, 437 (2008).
13. V. H. Pham, Y. H. Lee, D. J. Lee and J. S. Chung, *Korean J. Chem. Eng.*, **26**, 1585 (2009).
14. M. Bompart and K. Haupt, *Aust. J. Chem.*, **62**, 751 (2009).
15. F. Vandevele, A. S. Belmont, J. Pantigny and K. Haupt, *Adv. Mater.*, **19**, 3717 (2007).
16. H. Khan and J. K. Park, *Biotechnol. Bioprocess Eng.*, **11**, 503 (2006).
17. Yoshimatsu, K. Reimhult, A. Krozer, K. Mosbach, K. Sode and L. Ye, *Anal. Chim. Acta*, **584**, 112 (2007).
18. F. P. Capote, L. Ye, S. Shakil, S. A. Shamsi and S. Nilsson, *Anal. Chem.*, **80**, 2881 (2008).
19. J. Lee and J. K. Park, *Korean J. Chem. Eng.*, **26**, 453 (2009).
20. A. Ellwanger, C. Berggren, S. Bayoudh, C. Crencenzi, L. Karlsson, P. K. Owens, K. Ensing, P. Cormack, D. Sherrington and B. Sellergren, *Analyst*, **126**, 784 (2001).
21. P. J. Wu, J. Yang, Q. D. Su, Y. Gao, X. L. Zhu and J. B. Cai, *Chin. J. Anal. Chem.*, **35**, 484 (2007).
22. L. Schweitz, P. Spiegel and S. Nilsson, *Electrophoresis*, **22**, 4053 (2001).
23. M. G. Gallegos, R. M. Olivas and C. Cámara, *J. Environ. Manage.*, **90**, S69 (2009).
24. P. Spégel, L. Schweitz and S. Nilsson, *Electrophoresis*, **22**, 3833 (2001).
25. J. K. Park and J. W. Lee, *Korean J. Chem. Eng.*, **22**, 927 (2005).
26. C. R. Shelke, P. S. Kawtikwar, D. M. Sakarkar and N. P. Kulkarni, *Latest Reviews*, **6**, (2008).
27. G. Socrates, *Infrared characteristic group frequencies*, second edition, John Wiley & Sons Ltd., ISBN 0471942308 (1994).
28. D. Vaihinger, K. Lndfester, I. Krauter, H. Brunner and G. E. M. Tovar, *Macromolecular Chem. Phys.*, **203**, 1965 (2002).
29. R. G. Earnshaw and C. A. Price, *J. Appl. Polym. Sci.*, **32**, 5337 (1986).
30. A. G. Mayes and K. Mosbach, *Anal. Chem.*, **68**, 3769 (1996).
31. C. Jantararat, N. Tangthong, S. Songkro, G. P. Martin and R. Suedee, *Int. J. Pharm.*, **349**, 212 (2008).
32. S. Vidyasankar, M. Ru and F. H. Arnold, *J. Chromatogr. A*, **775**, 51 (1997).
33. Y. Liao, W. Wang and B. Wang, *Bioorganic Chem.*, **26**, 309 (1998).
34. M. Boopathi, M. V. S. Suryanarayana, A. K. Nigam, P. Pandey, K. Ganesan, B. Singh and K. Sekhar, *Biosens. Bioelectron.*, **21**, 2339 (2006).
35. J. M. Lin, T. Nakagama, K. Uchiyama and T. Hobo, *Chromatography*, **43**, 585 (1996).
36. L. Zhang, G. Cheng and C. Fu, *React. Funct. Polym.*, **56**, 167 (2003).
37. Y. Chen, M. Kele, I. Quinones, B. Sellergren and G. Guiochon, *J. Chromatogr. A*, **927**, 1 (2001).
38. N. Ul-Haq, T. Khan and J. K. Park, *J. Chem. Technol. Biotechnol.*, **83**, 524 (2008).